

AE4314 Helicopter Performance, Stability and Control
TU Delft online course

sylvain.pluchart@gmail.com

February 2020

Assignment I

Helicopter Description and Induced Velocity Calculations

1 Choose a helicopter

I choose to study the Boeing AH-64 Apache throughout the course. It is an american twin-turboshaft, four bladed, attack helicopter. Its development started in 1975 by the Hughes Helicopter company, acquired in 1984 by McDonnell Douglas. Since 1997 the production continues under the Boeing Defense, Space & Security umbrella.



Figure 1: AH-64D Apache Longbow firing during an inter army exercise in Bavaria (from wikimedia)

Table 1 summarizes the AH-64 version performance characteristics gathered from [janes.com](#) archive. We will consider in this study the AH-64A version, with T700-GE-701 engines, and without *longbow* (radar mounted on top of the main rotor).

Weights and Loadings

Empty weight	5165 kg (11387 lb)
Max. fuel weights:	
- internal	1108 kg (2442 lb)
- external (four Brunswick tanks)	2712 kg (5980 lb)
Max. Take-Off (MTOW)	9525 kg (21000 lb)
Max. disc loading	60.1 kg/m ² (12.31 lb/sq.ft)
<hr/>	
Performance at 6552 kg (14445 lb) gross weight (except for values given with external fuel)	
<hr/>	
Never-exceed speed (VNE)	197 kt (365 km/h; 227 mph)
Max. level and max. cruising speed	158 kt (293 km/h; 182 mph)
Max. vertical rate of climb at Sea Level	762 m (2500 ft)/min
<hr/>	
Service ceiling	6400 m (21000 ft)
Service ceiling, One Engine Inoperative	3290 m (10800 ft)
Hovering ceiling:	
- In Ground Effect (IGE)	4570 m (15000 ft)
- Out of Ground Effect (OGE)	3505 m (11500 ft)
<hr/>	
Max. range, internal fuel: 30 min reserves	260 n miles (482 km; 300 miles)
Ferry range, max. internal and external fuel, still air, 45 min reserves	1024 n miles (1899 km; 1180 miles)
Endurance at 1220 m (4000 ft) at 35 degC	1 h 50 min
Max. endurance:	
- internal fuel	2.7 hours
- internal and external fuel	8 hours
<hr/>	
g limits at low altitude and airspeeds up to 164 kt (304 km/h; 189 mph)	+3.5/-0.5

Table 1: AH-64A (without longbow) performance characteristics

2 Compare the chosen helicopter to existing designs

With a maximum take-off weight of 21000 lb, the AH-64 could be classified as a medium-lift helicopter. In terms of weight class and role, it is comparable to the rotorcrafts listed in Table 2 with some of their performance characteristics.

Powerplant All designs rely on twin-turboshaft powerplants. This configuration offers high power output to perform critical combat maneuvers. But it also increases the safety in case of engine failure, which is likely considering the harsh conditions on battlefields (high temperatures, dust, anti-air missiles and so on).

The AH-65A has the lowest power-to-weight ratio. Note that this value is based on the 701 engine version of the GE T700 turboshaft. It was later replaced by the more powerful 701C version.

Main rotor The comparison shows that the AH-64A has the smaller main rotor diameter relative to its length. As it is the older design considered here, we can assume that blade design analysis and manufacturing were not as advanced as they were for the others. Unsurprisingly we see that the rotor loading is higher than the value found for the Tigre or the Mi-28. Mostly because the Tigre is lighter and the Mi-28 has a higher disc area.

Range The lighter designs (A129, Tigre and Z-10) offer the highest range. The A129 is not as good as the Tigre and the Z-10 on that metric but we can assume that the older design of the powerplant (first flight in 1983) explains the gap.

The Mi-8 and AH-64A have similar range but that metric is influenced by different factors: the Mi-28 benefits from a more recent powerplant design, the AH-64A has the ability to carry a big amount of fuel in external tanks.

Commercial name	AH-64 Apache	Mi-28	A129 Mangusta	Tigre	Z-10
Manufacturer	Boeing Defense, Space & Security	NATO name "Havoc", Mil	Leonardo (ex. Augusta)	Airbus Helicopters (ex. Eurocopter)	Changhe Aircraft Industries Corporation (CAIC)
National origin	USA	Russia	Italy	Multinational (European program)	China
First flight	30 September 1975	15 October 2009	11 September 1983	27 April 1991	29 April 2003
Main rotor No. blades	4	5	5	4	5
<i>Dimensions</i>					
Main rotor diameter (m)	14.63	17.2	11.9	13	12
Length (m)	17.73	17.01	12.28	14.08	14.15
Height (m)	3.87	3.82	3.35	3.83	3.85
<i>Weights and Loadings</i>					
Empty weight (kg)	5165	8590	2530	3060	5100
Max. fuel weight int. + ext. (kg)	1108 + 2712	1337 + 4*445	?	1080 + ?	?
MTOW (kg)	9525	11500	4600	6000	7000
Max. disc loading (kg/m ²)	60.1	49.5	?	38.3	?
Power to weight ratio (kW/kg)	0.24	0.31	0.28	0.32	0.29
<i>Performance</i>					
Max. speed (km/h)	293	320	278	315	270
Range (km)	482	435	510	800	800
Service ceiling (m)	6400	5700	4725	4000	6400
Rate of climb (m/min)	762	816	612	643	609
Max. endurance (hours)	8	?	?	?	?

Table 2: performance comparison between the AH-64A (without longbow) and other attack helicopters of the same weight class

3 Induced velocity

3.1 Induced velocity in hover

In hover, out of ground effect, the thrust of the main rotor equals the weight of the helicopter:

$$T = W \quad (\text{I.1})$$

The Disc Actuation Theory and the expression of the mass flow rate derived in [vHM02] yields another expression for the thrust:

$$T = 2\rho\pi R^2 v_i^2 \quad (\text{I.2})$$

Combining (I.1) and (I.2) we can write an expression for the induced velocity v_i :

$$(v_i)_{\text{hover}} = \sqrt{\frac{m_{\text{rotorcraft}} \cdot g}{2\rho\pi R^2}} \quad (\text{I.3})$$

For the AH-64A version presented in Table 1, in typical combat configuration ¹:

$$(v_i)_{\text{hover}}^{6552\text{kg}, SL} = 12.5 \text{ m/s} \quad (\text{I.4})$$

with $m_{\text{rotorcraft}} = 6552 \text{ kg}$; $g = 9.80665 \text{ N/kg}$; $\rho = 1.225 \text{ kg/m}^3$ (mean value at Sea Level, 15 degC); $R = 7.3 \text{ m}$.

3.2 Induced velocity in forward flight

In forward flight, the forward force is generated by the main rotor. For this case we calculate the induced velocity using the ACT under the Glauert hypothesis as presented in [vHM02]:

$$(v_i)_{\text{forward}} = \frac{m_{\text{rotorcraft}} \cdot g}{2\rho\pi R^2 V_R} \quad (\text{I.5})$$

with V_R resulting from the vector summation of the flight speed V and the induced velocity v_i . Applying this formula to an AH-64A cruising at $V_R \approx V = 265 \text{ km/h}$ yields:

$$(v_i)_{\text{forward}}^{6552\text{kg}, V265, SL} = 2.2 \text{ m/s} \quad (\text{I.6})$$

with $m_{\text{rotorcraft}} = 6552 \text{ kg}$; $g = 9.80665 \text{ N/kg}$; $\rho = 1.225 \text{ kg/m}^3$; $R = 7.3 \text{ m}$; $V_R = 73 \text{ m/s}$.

3.3 Haffner diagram

The equilibrium of forces in forward level flight, provided that the H-forces are neglected, yields an expression to estimate the helicopter angle of attack (see [vHM02] for the detailed reasoning):

$$\sin \alpha = \frac{D_{\text{par}}}{m_{\text{rotorcraft}} \cdot g} \quad (\text{I.7})$$

parasite drag estimation At that stage we need to estimate the *parasite drag*. We will use correlation between the weight of the helicopter and its equivalent flat plate area (figure 5.11 in [vHM02]). We will consider the AH-64A to be aerodynamically "unrefined", as it is meant to fly with external payloads such as missiles and additional fuel tanks. It gives an equivalent flat plate area $\sum (C_D S)_S = 3 \text{ m}^2$.

The resulting parasite drag is obtained by multiplying this equivalent flat plate area by the dynamic pressure:

$$D_{\text{par}} = \frac{1}{2} \cdot \sum (C_D S)_S \cdot \rho V^2 \quad (\text{I.8})$$

Combining (I.7) and (I.8) we can finally estimate the angle of attack for a level flight at $V = 265 \text{ km/h}$, Sea Level:

$$\alpha^{6552\text{kg}, V265, SL} \simeq 9 \text{ deg} \quad (\text{I.9})$$

(with the same numerical values as for (I.6)).

¹gross weight for anti-armour at 1220 m/4000 ft and 35degC, four Hellfire and 320 rounds of 30 mm ammunition, no external fuel.

induced velocity using the Haffner-diagram We read the induced velocity on the Haffner-diagram from the non-dimensional flight speed ($\bar{V} = \frac{V}{v_i} = \frac{73}{12.5} = 5.84$). It yield a non-dimensional induced velocity of $\bar{v}_i \approx 0.175$, which in turns yields an actual induced velocity of $v_i = 0.175 \cdot 12.5 \simeq 2.2 \text{ m/s}$.

The value we obtain with this method and the one calculated using the ACT under the Glauert hypothesis are similar. We would need to compute more operating conditions to see if that would be true for the entire range of operation (speeds and weights).

A level of uncertainty in using the Haffner-diagram comes from the estimation of parasite drag value (on top of reading the diagram itself!). We can assume that using experimental data for that in the AH-64A case gave us a good prediction because it is easier to classify it as aerodynamically "unrefined". It might be difficult to know which experimental data to use for cleaner fuselage shapes.

References

- [vHM02] Th. van Holten and A. Melkert. Helicopter performance, stability and control. faculty of aerospace engineering delft university of technology. AE4-213 lecture notes. Translation and revision of the original Dutch version by Ben Marrant and Marilena Pavel, 2002.

AE4314 Helicopter Performance, Stability and Control
TU Delft online course

sylvain.pluchart@gmail.com

February 2020

Assignment II

Helicopter performance calculations (power curves)

1 Power required to hover

In this section I will consider an AH-64A version with a gross weight of 6552 kg, hovering at Sea Level, out of ground effect.

1.1 ideal power

The ideal power to hover can be written as:

$$P_{\text{hover},id} = W \sqrt{\frac{W}{2\rho\pi R^2}} \quad (\text{II.1})$$

with $W = m_{\text{rotorcraft}} \cdot g$

$$(P_{\text{hover},id})^{6552\text{kg},SL} = 804 \text{ kW} \quad (\text{II.2})$$

with $m_{\text{rotorcraft}} = 6552 \text{ kg}$; $g = 9.80665 \text{ N/kg}$; $\rho = 1.225 \text{ kg/m}^3$; $R = 7.3 \text{ m}$.

1.2 ideal power in ACT theory

Figure of Merit The actual power needed to hover following the ACT theory is obtained by dividing the ideal power by a *Figure of Merit* (*FM*), usually taking a value between 0.6 and 0.8:

$$P_{\text{hover,ACT}} = \frac{P_{\text{hover},id}}{FM} \quad (\text{II.3})$$

To define the FM value for the AH-64's main rotor, we will use experimental data on 0.27-scale rotor presented in a 1990 NASA's report [Kel90]. In this study the baseline main rotor *FM* is given as a function of the non-dimensional thrust coefficient C_T , for different blade tip Mach numbers M_t .

First I need to calculate the blade Mach tip number and the thrust coefficient as defined in [vHM02]:

$$M_t = \frac{\Omega R}{c^{15degC,SL}} = \frac{221.3 \text{ m/s}}{340.27 \text{ m/s}} = 0.65 \quad (\text{II.4})$$

$$(C_T)^{6552\text{kg},SL} = \frac{T}{\rho(\Omega R)^2 \pi R^2} = 6.4 \cdot 10^{-3} \quad (\text{II.5})$$

with $T = W$, $\Omega R = 221.3 \text{ m/s}$ and all other values as in (II.2).

I read on Figure 1 a value of $FM = 0.7$. I can now calculate the power to hover under the ACT:

$$(P_{\text{hover,ACT}})^{6552\text{kg},SL} = 1149 \text{ kW} \quad (\text{II.6})$$

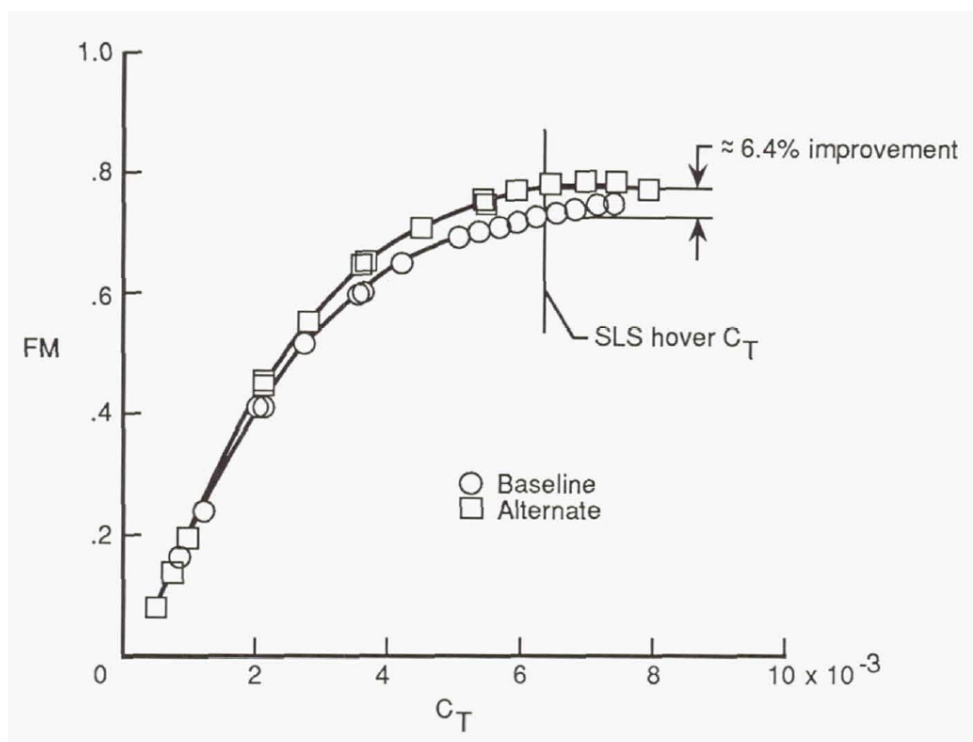


Figure 1: Rotor FM in hover at $M_t = 0.64$, baseline and alternate design, from [Kel90]

1.3 ideal power in BEM theory

expression of power to hover from the BEM As derived during the lecture on BEM, the power to hover can be written as:

$$P_{\text{hover},\text{BEM}} = P_i + P_p = kT v_i + \sigma \frac{\overline{C}_{Dp}}{8} \rho (\Omega R)^3 \pi R^2 \quad (\text{II.7})$$

correction factor for the induced power k is a correction factor that takes into account the non-uniformity of the induced velocity and the small rotation in the wake. It is usually taken to be between 1.1 and 1.2. To be consistent with the charts presented in the lecture notes [vHM02], I will use a value of $k = 1.15$.

solidity of the rotor It is design parameter defined as the ratio of blade area divided by the total area:

$$\sigma = \frac{Nc}{\pi R} = 0.09 \quad (\text{II.8})$$

with $N = 4$ (number of blades); $c = 0.53 \text{ m}$ (blade chord); $R = 7.3 \text{ m}$.

mean blade drag coefficient I obtained a first estimation of the mean blade drag coefficient using Xfoil (Figure 2), telling me that I should use a value around $\overline{C}_{Dp} \approx 0.01$ for small angles of attack.

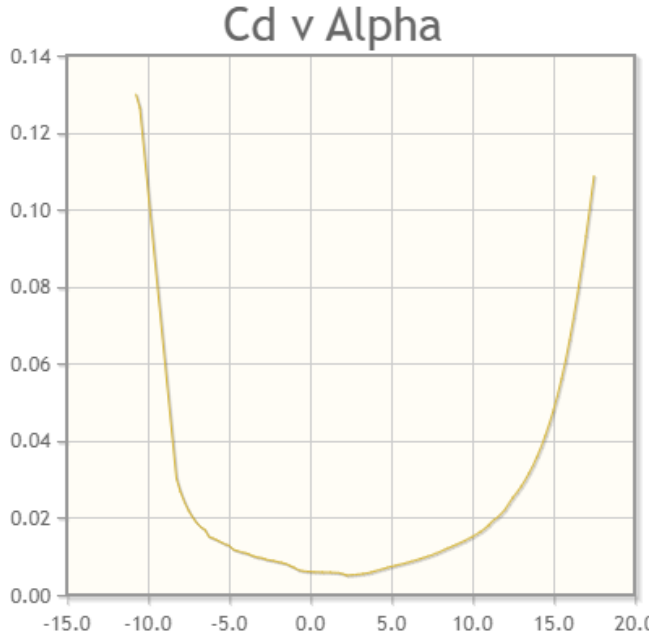


Figure 2: CD profile versus angle of attack for a HH-02 airfoil. Generated by Xfoil for high Reynolds number ($Re \approx 10^6$)

To confirm this estimation I first used the values of the thrust coefficient and rotor solidity computed in (II.5) and (II.8) to compute the mean lift coefficient C_L :

$$\overline{C}_L = \frac{6.6 \cdot C_T}{\sigma} = 0.47 \quad (\text{II.9})$$

The chart Figure 3.7 in [vHM02] gives the mean drag coefficient as a function of the blad tip Mach and the mean lift coefficient. Using that method I end up with the same estimation as the one obtained with Xfoil. I will then use $\overline{C}_{Dp} = 0.01$ for the hover power calculation.

I now have enough information to compute the power to hover with equation (II.7):

$$(P_{\text{hover},\text{BEM}})^{6552kg,SL} = 1182 \text{ kW} \quad (\text{II.10})$$

with numerical values similar to all previous calculations.

2 Power required in level flight - graphical representation as a function of velocity (power curve)

2.1 helicopter rotor power in level flight

The helicopter main rotor power request in forward level flight (the subscript 0 indicates a level flight) can be written as a sum of different contributions (see section 5.9 in [vHM02]):

$$P_{t0} = \underbrace{P_i}_{\text{induced power}} + \underbrace{P_p + P_d}_{\text{profile drag power}} + \underbrace{P_{par}}_{\text{parasite drag power}} \quad (\text{II.11})$$

induced power The expressions for P_i is similar to the hover case (II.7).

profile drag power The first term P_p is same as the one in the hover case (II.7). The second term P_d takes a similar form, with the addition of a factor $n\mu^2$ in front of the expression. μ is the tip speed ratio ($\mu = V/\Omega R$) and n is a parameter that itself depends the tip speed ratio. I will use a value of $n = 4.65$ as indicated in the lecture notes.

parasite drag power In assignment1 I have computed the parasite drag D_{par} . I will reuse the same expression for the parasite drag power calculation:

$$P_{par} = D_{par}V = \frac{1}{2} \cdot \sum (C_D S)_S \cdot \rho V^3 \quad (\text{II.12})$$

The final expression for the power request is:

$$P_{t0} = kW v_i + \sigma \frac{\overline{C_{Dp}}}{8} \rho (\Omega R)^3 \pi R^2 (1 + 4.65\mu^2) + \frac{1}{2} \cdot \sum (C_D S)_S \cdot \rho V^3 \quad (\text{II.13})$$

induced velocity In assignment1 I used the ACT (under the Glauert assumption, usable for high forward flight speed) and the Haffner diagram to compute the induced velocity in forward flight. For this assignment I will use the approximations for low and high-speed flight presented Figure 5.8 in [vHM02].

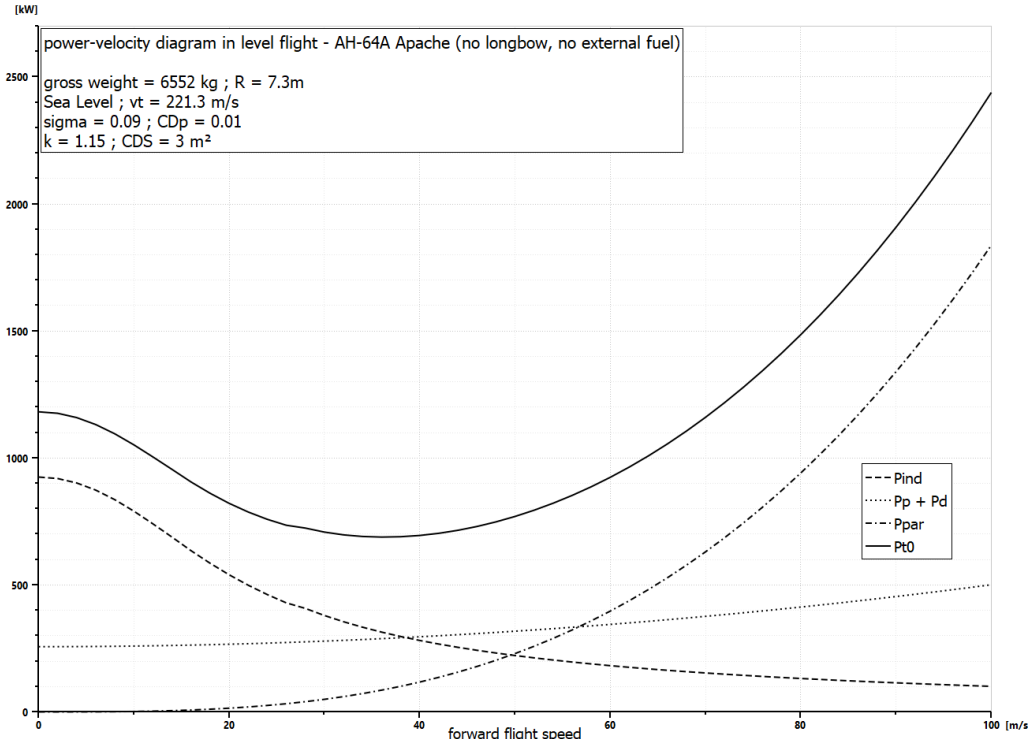


Figure 3: Power-velocity diagram for the helicopter, tail rotor not taken into consideration

2.2 tail rotor power P_{tr} in level flight

The power-velocity diagram of the tail rotor is built following the main rotor's method. An additional factors accounting for the vertical fin blockage of 1.1 will be used to compute the power request. The correction factor k_{tr} for the induced power, similar to the one define in the main rotor case (II.7), will be set to 1.3.

Figure 4 shows the power profile obtained for the tail rotor.

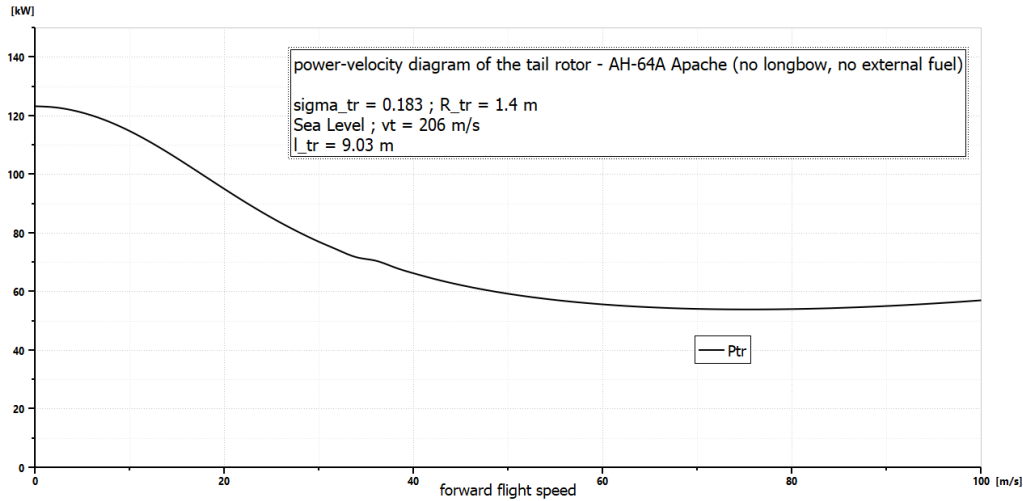


Figure 4: Power-velocity diagram for the tail rotor

2.3 power-velocity diagram

Figure 3 shows the power-velocity diagram built from (II.13). All parameters are already known from the previous study in hover condition.

3 Speed for maximum endurance and speed for maximum range

3.1 performance diagram and characteristic speeds

performance diagram Figure 5 shows the performance diagram built from the total power request $P_{t_0} + P_{tr}$, on top of the engines maximum power P_e and engines available power P_a . In order to compare with values from the literature (janes.com archive), I computed the power request for a flight at 1220 m (4000 ft), at 35 degC.

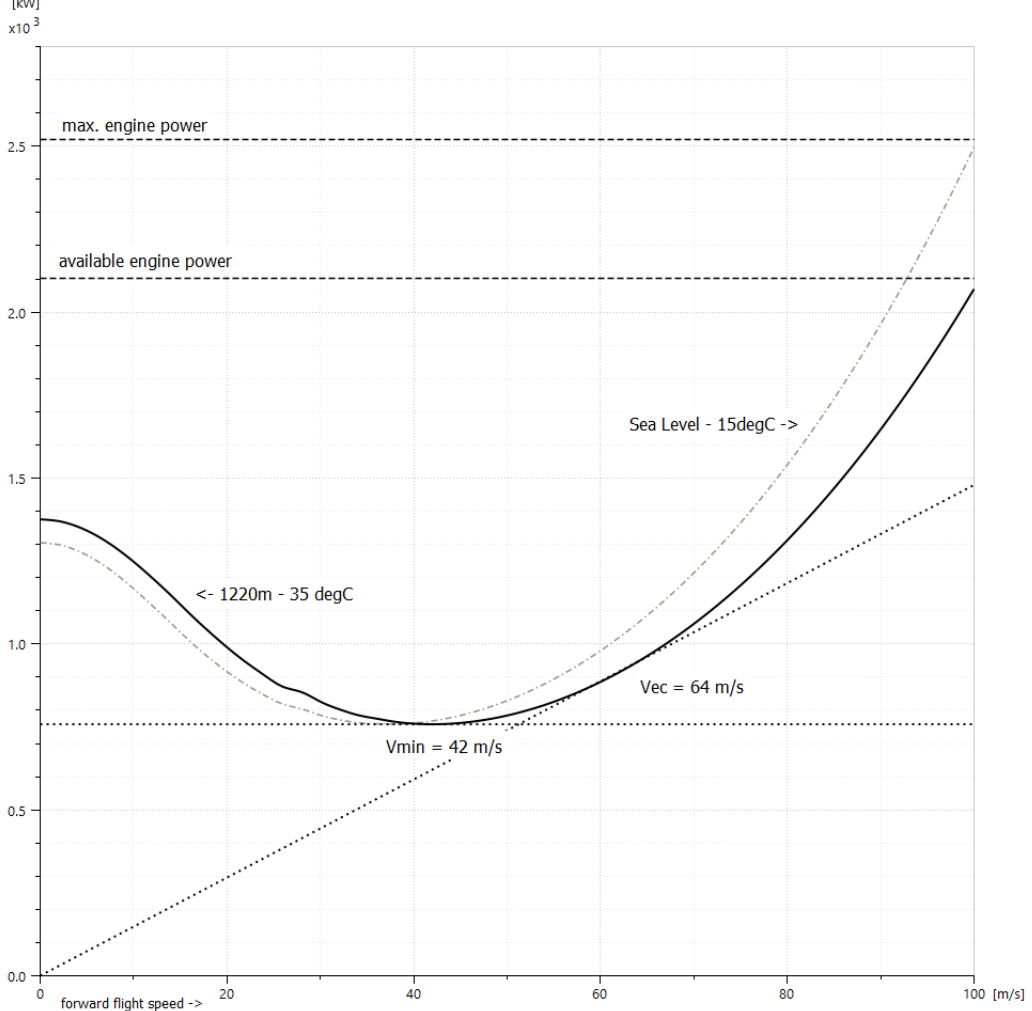


Figure 5: Performance Diagram of the AH-64A Apache (no longbow, no external fuel), with $P_e = 2520 \text{ kW}$ (max. Take-Off rating) and $P_a = 0.834 \cdot P_e$

characteristic flight speeds Table 1 lists three characteristic flights speeds from the performance diagram.

performance diagram	level condition	speed value in m/s (km/h)
$v_{p_{min}}$ (point A)	minimum power (minimum fuel use)	42 (151)
v_{ec} (point B)	maximum specific flight range	64 (230)
v_{max} (point C)	maximum speed	102 (367)

Table 1: AH-64A (without longbow) performance characteristics, gross weight 6552 kg, at 1220m and 35 degC

3.2 comparison with public performance data

I did not find values of $v_{p_{min}}$ and v_{ec} in public data I could compare my estimation with. But other data are easily accessible for the configuration considered. Values useful to my study are listed in Table 2 (janes.com archive).

mission fuel m_{fuel}	727 kg (1602 lb)
turboshaft specific fuel consumption $SFC_{T700-GE-701}$	0.263 kg/kW · hr (0.433 lb/hp · hr)
max. range (with 30 min. reserve)	482 km (260 nm)
virtually extended max. range (no reserve)	597 km (322 nm)
max. endurance (mean value from different public sources)	3 hr
max.speed v_{max}	293 km/h (158 kn)
never-exceed speed v_{NE}	365 km/h (197 kn)

Table 2: AH-64A (without longbow) public data used to compare estimated values of $v_{p_{min}}$ and v_{ec} (same configuration as for Table 1).

speed for minimum power $v_{p_{min}}$ Combining the specific fuel consumption of the turboshaft from Table 2, the predicted Power Request $(Pr_{min})^{6552kg,1220m,35degC}$ at $v_{p_{min}}$ from Figure 5, I can estimate the max. endurance:

$$(max.endurance)_{estimated} = \frac{m_{fuel} \cdot (Pr_{min})^{6552kg,1220m,35degC}}{SFC_{T700-GE-701}} = 3.6 \text{ hr} \quad (\text{II.14})$$

The value obtained is higher than the 3hr value found in various sources. It could mean that I underestimated the power request in my calculation. But one should look at this comparison with care:

- It is not clear whether the value of max. endurance found in public data includes a 30 min reserve. If we consider a 30 min. reserve, then my power request prediction is in line with the AH-64A actual performance.
- I neglected here the fact that the rotorcraft weight is varying during the mission as it burns fuel on board. If we do so the power request would decrease compared to the 6552 kg version.
- I also neglected the extra power needed to take-off and reach the mission altitude and speed. Adding this extra power would decrease the max. endurance value estimated.

speed for max. range v_{ec} Combining the specific fuel consumption of the turboshaft and the max. range from Table 2, the predicted Power Request $(Pr_{ec})^{6552kg,1220m,35degC}$ and speed v_{ec} from Figure 5, I can estimate the fuel mass to reach max. range:

$$m_{fuel} = \frac{\text{max. range (no reserve)}}{v_{ec}} \cdot (Pr_{ec})^{6552kg,1220m,35degC} \cdot SFC_{T700-GE-701} = 646 \text{ kg} \quad (\text{II.15})$$

The value seems to be underestimated when compared to the 727 kg found in public data. Similarly to the max. endurance calculation, I neglected the extra power needed to take-off and reach the mission altitude and speed. Doing so would increase the estimated m_{fuel} .

max.speed v_{max} The value obtained with the performance diagram seems overestimated as it is close to the never-exceed speed v_{NE} , when I would have expected a value around 293 km/h as found in public data. I also know that the 300 km/h limit is typical for conventional rotorcrafts. Few designs would lead to higher values, by including wings or pusher propellers for instance. I see two potential explanations to this discrepancy:

- The estimation of the max. endurance and the max. range showed that my power request seems to be in both cases underestimated. A higher power request would lead to a lower value of v_{max} , more in line with the actual performance of the AH-64A.
- The maximum forward flight does not only depend on the max. available power, but also depends on:
 - the main rotor blade tip Mach number $M_{tip} < 0.85$ (compressibility of the advancing blades),
 - and the advance ratio $\mu < 0.4$ (stall limit of the retreating blades).

Applying these two criteria to my configuration of the AH-64A yields:

$$(v_{max})_{advancing} < a \cdot 0.85 - \Omega R = 77.8 \text{ m/s (280 km/h)} \quad (\text{II.16})$$

and:

$$(v_{max})_{retreating} < 0.4 \cdot \Omega R = 88.5 \text{ m/s (317 km/h)} \quad (\text{II.17})$$

The criteria on the compressibility of the advancing blade would limit the maximum forward speed to a value close to the actual limit of the AH-64A. It seems to be the limiting one here, and not the available power.

note on the engine power available The engine power available seems high compared to the actual limits of the main rotor in forward flight. In my opinion it can be explained by the type of mission the AH-64A was designed for. When engaged on the battlefield, extra power might be needed for good maneuvering (climb, accelerate and so on) and for additional safety (need to fly with one engine inoperative). On top of that, as presented in Assignment 1, the gross weight of the AH-64A can reach a value of 9525 kg (by adding for instance up to 2712 kg of fuel in external tanks), thus requiring additional power to fulfill the mission.

References

- [Kel90] Henry L. Kelley. Aerodynamic performance of a 0.27-scale model of an ah-64 helicopter with baseline and alternate rotor blade sets. Technical report, 1990. Aerostructures Directorate USAARTA-AVSCOM Langley Research Center Hampton, Virginia.
- [vHM02] Th. van Holten and A. Melkert. Helicopter performance, stability and control. faculty of aerospace engineering delft university of technology. AE4-213 lecture notes. Translation and revision of the original Dutch version by Ben Marrant and Marilena Pavel, 2002.

AE4314 Helicopter Performance, Stability and Control
TU Delft online course

sylvain.pluchart@gmail.com

February 2020

Assignment III

Rotor Flapping Dynamics

1 Helicopter hovering

In this section I will consider an AH-64A version with a gross weight of 6552 kg, hovering at Sea Level, out of ground effect.

1.1 flapping angle in the rotating frame

1.1.1 flapping equation, non-dimensional quantities, blade pitch and angle of attack

The momentum balance on a blade element, with gravity effect being neglected, leads to the flapping equation:

$$\ddot{\beta} + \Omega^2\beta = \frac{M_a}{I} \quad (\text{III.1})$$

As done in section 9. of the lecture notes [vHM02], the contribution of the aerodynamic force on the blade element is detailed to rewrite the flapping equation in the hover case with no fuselage motion:

$$\ddot{\beta} + \frac{\gamma}{8}\Omega\dot{\beta} + \Omega^2\beta = \frac{\gamma}{8}\Omega^2 \left(\theta_0 - \frac{4}{3}\lambda_i \right) \quad (\text{III.2})$$

With two non-dimensional quantities defined as:

$\lambda_i = \frac{v_i}{\Omega R}$ is the non-dimensional induced velocity, or *inflow ratio*.

$\gamma = \frac{\rho C_{L\alpha} c R^4}{T}$ is the *Lock number*, a measure of the balance between aerodynamic and inertial forces on the rotor.

blade lift coefficient derivative with respect to angle of attack $C_{L\alpha}$ I obtained a first estimation of the lift derivative coefficient with respect to angle of attack using Xfoil (Figure 1). I will use $C_{L\alpha} = 0.12/\text{degree} = 6.88/\text{rad}$.

angle of attack α I computed the blade angle of attack from the thrust expression in Blade Element Theory (BEM) established in a previous lecture:

$$T = N \int_0^R dT \approx N \int_0^R dL = N \frac{\rho}{2} \int_0^R C_L(\Omega r)^2 c dr \quad (\text{III.3})$$

From this integral I established an expression for α (III.4), based on the following assumptions:

- the chord c is constant along the radius,
- the pitch angle θ is constant along the radius,
- the lift is generated between the root ($r = 0$) and the effective radius ($Re = 0.97 \cdot R$),
- $C_L = C_{L\alpha} \cdot \alpha$.

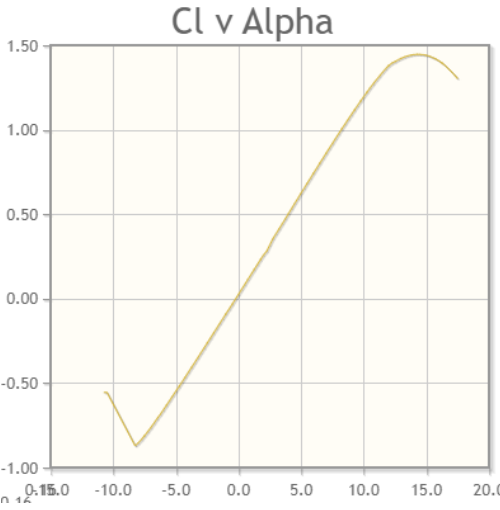


Figure 1: CL profile versus angle of attack for a HH-02 airfoil. Generated by Xfoil for high Reynolds number ($Re \approx 10^6$)

$$\alpha = \frac{6 \cdot W}{N\rho C_{L\alpha} \Omega^2 c Re^3} = 3.8 \text{ deg} \quad (\text{III.4})$$

with $m_{rotorcraft} = 6552 \text{ kg}$; $g = 9.80665 \text{ N/kg}$; $\rho = 1.225 \text{ kg/m}^3$; $R = 7.3 \text{ m}$; $C_{L\alpha} = 6.88 \text{ 1/rad}$; $N = 4$; $\Omega = 30.3 \text{ rad/s}$.

remark This value of α gives a mean lift coefficient of $\bar{C}_L = C_{L\alpha} \cdot \alpha = 0.12 \cdot 3.8 = 0.46$. It is consistent with the value $\bar{C}_L = 0.47$ used in assignment 1 and 2.

AH-64A Lock number Let's compute the Lock number for the AH-64A, at Sea Level.

$$\gamma = \frac{1.225 \text{ kg/m}^3 \cdot 6.88 \cdot 0.53 \text{ m} \cdot (7.3 \text{ m})^4}{(5152/4) \text{ kgm}^2} = 9.8 \quad (\text{III.5})$$

collective pitch θ_0 The flight velocity components and the associated angles as defined in the lecture gives:

$$\theta_0 = \alpha + \text{atan} \left(\frac{v_i}{\Omega R} \right) \approx \alpha + \lambda_i = 7 \text{ deg} \quad (\text{III.6})$$

with $v_i = 12.5 \text{ m/s}$ in hover (other parameters unchanged).

1.1.2 flapping equation implementation

In order to ease the analysis of the flapping dynamics in the future, for the hover case but also for other operating conditions, I choose to implement the flapping equation III.2 in Simcenter Amesim , part of the Siemens Simcenter software suite. It is a tool specialized in system dynamics modeling and simulation. Some of its feature will be useful to the flapping dynamic analysis, such as:

- a robust solver for systems of differential equations,
- a set of pre- and post-processing capabilities,
- an existing database of atmosphere models and other physical models useful in aircraft modeling,
- a set of linear analysis tools (frequency domain analysis).

state-space representation To create a rotor component in Simcenter Amesim , I will first rewrite the flapping equation as *state-space representation* of the the system. It means that instead of solving a 2nd-order differential equation, I will create a system made of two 1st-order differential equations:

$$III.2 \Leftrightarrow \begin{cases} \dot{B} + \frac{\gamma}{8}\Omega B + \Omega^2 \beta = \frac{\gamma}{8}\Omega^2 (\theta_0 - \frac{4}{3}\lambda_i) \\ B = \dot{\beta} \end{cases} \Leftrightarrow \begin{bmatrix} \dot{B} \\ \dot{\beta} \end{bmatrix} = \begin{bmatrix} -\frac{\gamma}{8}\Omega & -\Omega^2 \\ 1 & 0 \end{bmatrix} \cdot \begin{bmatrix} B \\ \beta \end{bmatrix} + \begin{bmatrix} \frac{\gamma}{8}\Omega^2 (\theta_0 - \frac{4}{3}\lambda_i) \\ 0 \end{bmatrix} \quad (\text{III.7})$$

B and β are the *state variables* of the system.

The state representation $\dot{X} = AX + B$ has many advantages. The first one is that numerical algorithms available to integrate differential equations are designed to handle 1st-order equations. The second advantage of this description is the ability to use linear analysis tools. The matrix A for instance will give us many useful information on the system's dynamics (its eigenfrequencies for instance).

TODO(Sylvain): insert screenshots of the Amesim implementation?

1.1.3 application to the AH-64A in hover

Using the quantities calculated in previous section and the flapping equation implementation, we can solve it for the AH-64A in hover at Sea Level.

transient $\beta_{hom}(t)$ The transient motion, when the initial flapping angle is moved away from its equilibrium value, is quickly damped. Figure 2 shows the homogeneous solution $\beta_{hom}(t)$ for two rotations.

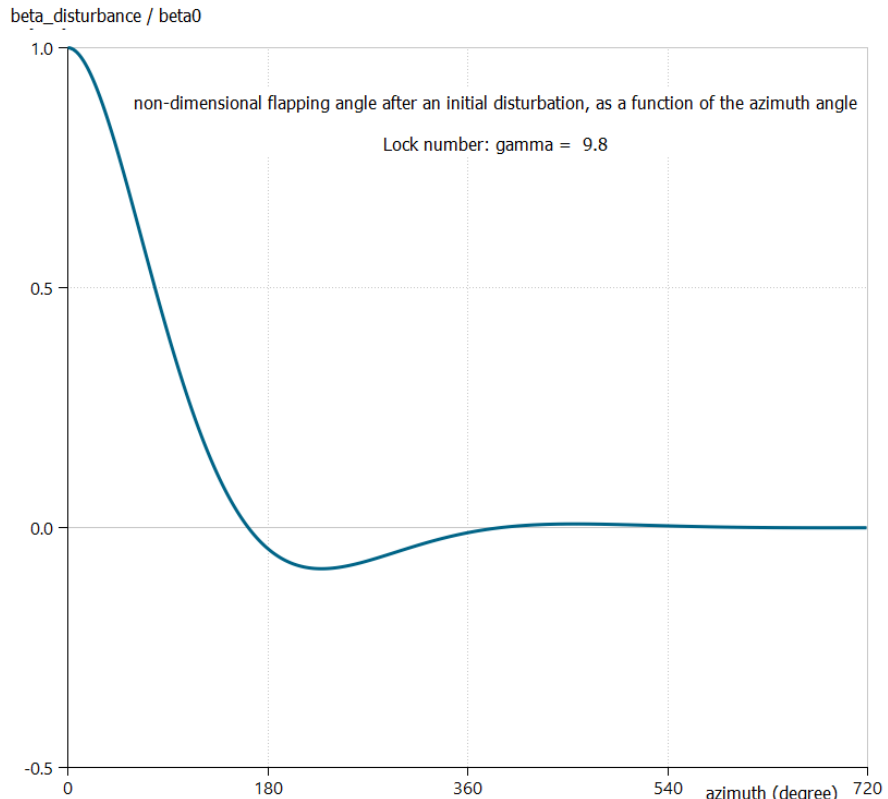


Figure 2: Non-dimensional flapping angle evolution after an initial perturbation

equilibrium state $\beta_{part}(t)$ The particular solution of the flapping equation corresponds to a constant flapping angle, the *coning angle* of the rotor. The values displayed in the variables panel Figure 3 corresponds to a stabilizing run. Simcenter Amesim looks for an equilibrium position when one exists. The value calculated is $\beta_0 \simeq 3.3 \text{ deg}$.

TODO(Sylvain): add linear analysis screenshot, like eigenfrequency

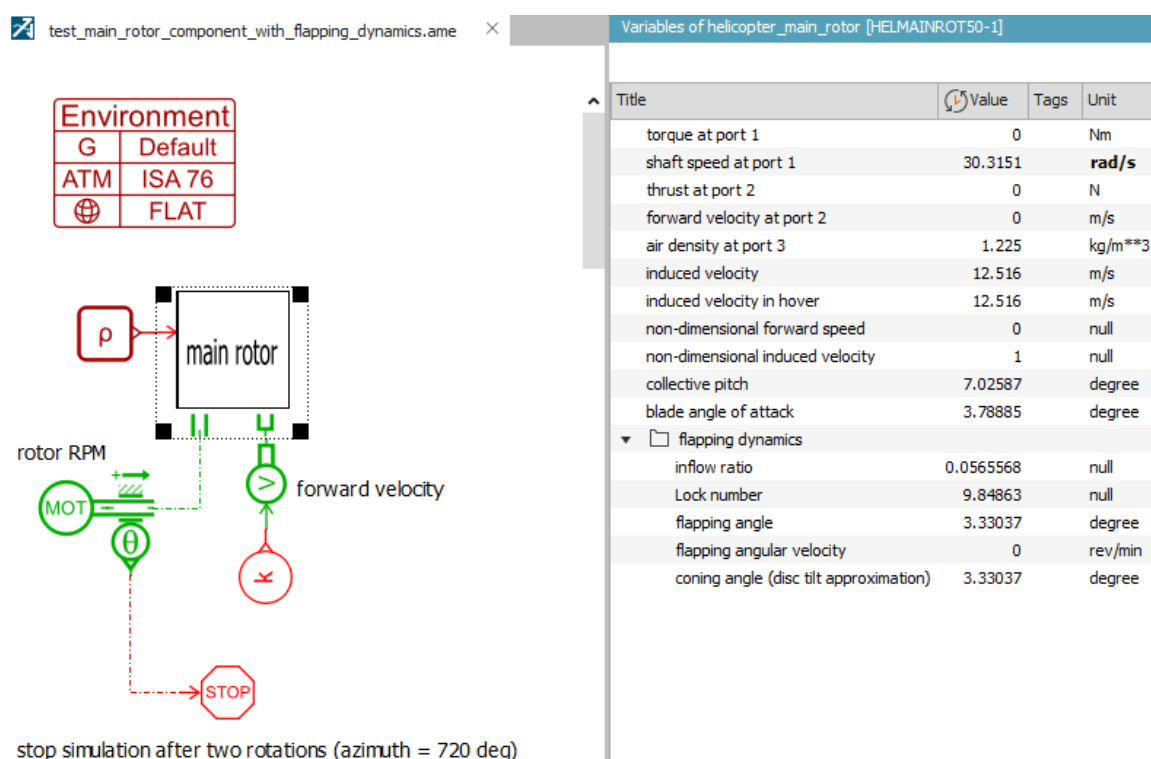


Figure 3: Results of a stabilizing run in Simcenter Amesim

1.2 flapping angle in the non-rotating frame (disc tilt approximation)

As presented during the lecture there is a disc approach to study the flapping motion. It is obtained by a Fourier series applied to the flapping motion, to transform it from rotating to the non-rotating plane:

$$\beta = a_0 - a_1 \cos(\psi) - b_1 \sin(\psi) \quad (\text{III.8})$$

- a_0 coning angle
- a_1 longitudinal disc tilt
- b_1 lateral disc tilt

In hovering flight longitudinal and lateral tilt are zero. For the hover case I only need to calculate the coning angle a_0 . As expected the value is the one that we obtained by computing the particular solution of the flapping equation III.2.

$$a_0 = \frac{\gamma}{8} \left(\theta_0 - \frac{4}{3} \lambda_i \right) = 3.3 \text{ deg} \quad (\text{III.9})$$

2 Helicopter fixed to the ground with body pitch rate

2.1 flapping angle in the rotating frame

flapping equation with body pitch rate I will start from the flapping equation of motion, when the helicopter has a body rate q in hover, from the lecture notes:

$$\ddot{\beta} + \frac{\gamma}{8}\Omega\dot{\beta} + \Omega^2\beta = \underbrace{-2q\Omega\sin(\psi)}_{\text{coriolis effect}} + \underbrace{\frac{\gamma}{8}q\Omega\cos(\psi)}_{\text{aerodyn. effect of } q} + \underbrace{\frac{\gamma}{8}\Omega^2\left(\theta_0 - \frac{4}{3}\lambda_i\right)}_{\text{aerodyn. effect of lift}} \quad (\text{III.10})$$

effect of body roll rate The effect of a body roll rate p on the flapping motion will be similar to the expressions established for the pitch rate effect q . The effect will be applied with a phase shift of $\frac{\pi}{2}$ rad compared to the pitch rate. I will then rewrite equation III.10 to take that additional effect into account:

$$\ddot{\beta} + \frac{\gamma}{8}\Omega\dot{\beta} + \Omega^2\beta = \underbrace{-2\Omega[q\sin(\psi) - p\cos(\psi)]}_{\text{coriolis effect}} + \underbrace{\frac{\gamma}{8}[q\cos(\psi) + p\sin(\psi)]}_{\text{aerodyn. effect of } q \text{ and } p} + \underbrace{\frac{\gamma}{8}\Omega^2\left(\theta_0 - \frac{4}{3}\lambda_i\right)}_{\text{aerodyn. effect of lift}} \quad (\text{III.11})$$

Figure 4 shows a blade flapping angle evolution for one revolution and different combinations of pitch and roll rate. The results are shown after transient due the initial value of flapping angle has vanished. All values taken for an AH-64A in hover at Sea Level.

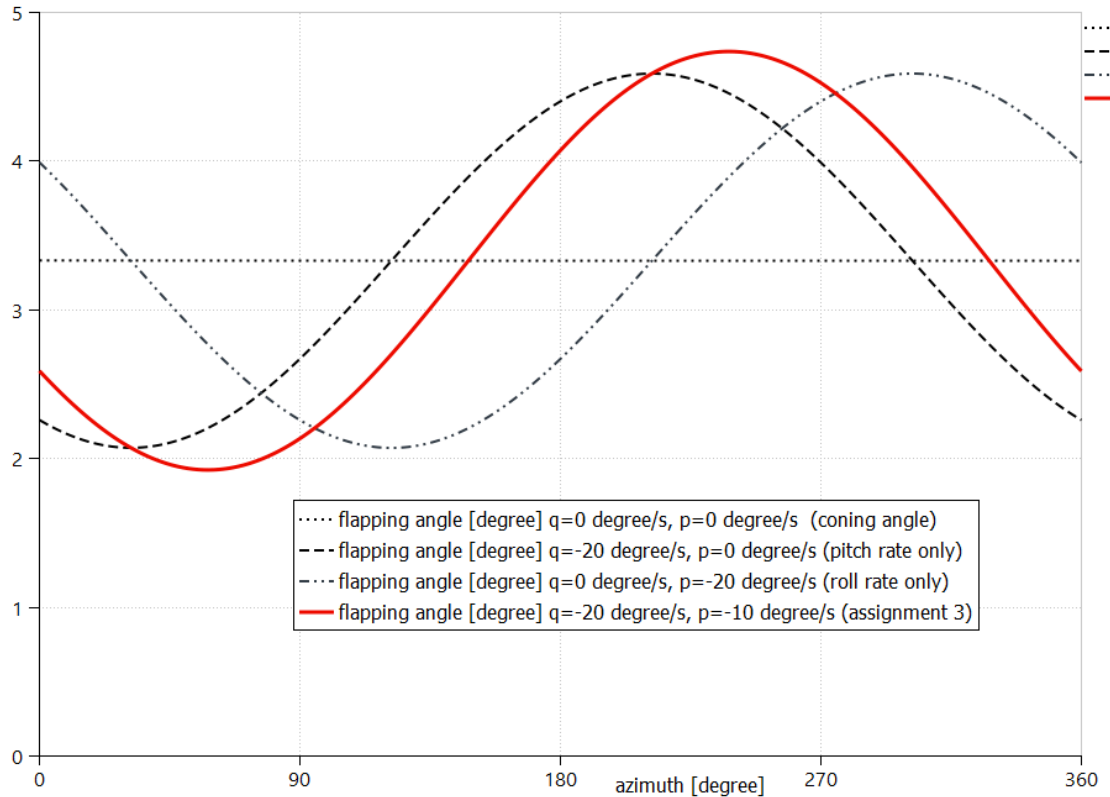


Figure 4: Flapping angle evolution over one revolution, with different combination of pitch and roll rate

comments on the results From Figure 4 we see that:

- As expected, the adapted differential equation III.11 has the same particular solution as the one calculated in the hover case, which is the coning angle.
- When performing a body nose down maneuver ($q < 0 \text{ deg/s}$ and $p = 0 \text{ deg/s}$) the tip path plane tilts backward. As explained in [vHM02] it shows that the tip path plane lags the rotation of the control plane, which damps the body motion.

- For this nose down maneuver, the tip path plan also tilts laterally. It means that there is a coupling between the symmetric and asymmetric motion of the helicopter.
- When performing a roll maneuver "to the left" (starboard up, $q = 0 \text{ deg/s}$ and $p < 0 \text{ deg/s}$), we see as expected the same disc response as for a pitch only maneuver, with a $\frac{\pi}{2} \text{ rad}$ offset.

2.2 flapping angle in the non-rotating frame (disc tilt approximation)

I will use here the disc tilt approximation III.8, where the coefficients a_1 and b_1 are no longer equal to 0 (longitudinal and lateral tilt). Substituting it into the flapping equation with body pitch and roll rate III.11 allows me to build expressions for a_1 and b_1 and calculate their value for $p = -20 \text{ deg/s}$ and $q = -10 \text{ deg/s}$:

$$\begin{aligned} a_1 &= -\frac{16}{\gamma} \cdot \frac{q}{\Omega} + \frac{p}{\Omega} = 0.74 \text{ deg} \\ b_1 &= -\frac{16}{\gamma} \cdot \frac{p}{\Omega} - \frac{q}{\Omega} = 1.2 \text{ deg} \end{aligned} \quad (\text{III.12})$$

note for a counter-clockwise rotation of the main rotor

- A positive value of a_1 is a tilt backward (a negative body pitch rate $q < 0 \text{ deg/s}$ is a nose down maneuver).
- A positive value of b_1 is a tilt to the right, view from aft (a negative body roll $p < 0 \text{ deg/s}$ is a starboard up maneuver).

3 Helicopter in forward flight

forweword As derived in the lecture, the aerodynamic flapping moment in forward flight depends on the following non-dimensional quantities:

- the tip speed ratio $\mu = \frac{V \cos(\alpha_c)}{\Omega R}$,
- the inflow velocity perpendicular to the control plane $\lambda_c = \frac{V \sin(\alpha_c)}{\Omega R}$,
- the inflow ratio $\lambda_i = \frac{v_i}{\Omega R}$,
- the collective pitch θ ,
- and the pitch rate q .

To compute all these quantities, I need first to find the rotor angle of attack in the control plane α_c and the collective pitch θ in trim condition for the forward flight considered ($V = 20 \text{ m/s}$). I will implement the procedure to do that in the next assignment, where I will build a 3 degree-of-freedom flight simulator. For that study I will assume that the angle of attack α_c will take small values, so that $\cos(\alpha_c) \simeq 1$ and $\sin(\alpha_c) \simeq 0$. It means that I will consider $\lambda_c \simeq 0$.

3.1 flapping angle in the rotating frame

I will implement the flapping equation as established in the lecture notes:

$$\ddot{\beta} + \frac{\gamma}{8}\Omega\dot{\beta} \left[1 + \frac{4}{3}\mu \sin(\psi) \right] + \Omega^2\beta \left[1 + \frac{\gamma}{6}\mu \cos(\psi) + \frac{\gamma}{8}\mu^2 \sin(2\psi) \right] = \\ -2q\Omega \sin(\psi) + \frac{\gamma}{8}\Omega^2\theta(1 + \mu^2) - \frac{\gamma}{6}\Omega^2(\lambda_c + \lambda_i) + \frac{\gamma}{8}\Omega^2\mu \sin(\psi) \left(\frac{8}{3}\theta - 2(\lambda_c + \lambda_i) \right) \\ + \frac{\gamma}{8}\Omega^2\frac{q}{\Omega} \cos(\psi) + \frac{\gamma}{12}\Omega^2\frac{q}{\Omega} \mu \sin(2\psi) - \frac{\gamma}{8}\Omega^2\theta\mu^2 \cos(2\psi) \quad (\text{III.13})$$

The resulting flapping dynamics is presented Figure 5. I observe that:

- the rotor cone is blowing backward,
- the rotor is tilting to the right (asymmetry of the lift).

3.2 flapping angle in the non-rotating frame (disc tilt approximation)

I calculated the a_0 , a_1 and b_1 coefficients according to the expressions derived during the lecture:

$$a_0 = \frac{\gamma}{8} \left[\theta(1 + \mu^2) - \frac{4}{3}(\lambda_i + \lambda_c) \right] = 3.9 \text{ deg} \\ a_1 = \frac{-\frac{16}{\gamma} \cdot \frac{q}{\Omega} + \frac{8}{3}\mu\theta - 2\mu(\lambda_i + \lambda_c)}{1 - \frac{1}{2}\mu^2} = 1 \text{ deg} \\ b_1 = \frac{-\frac{q}{\Omega} + \frac{4}{3}\mu a_0}{1 + \frac{1}{2}\mu^2} + \frac{K'\lambda_i}{1 + \frac{1}{2}\mu^2} = 2 \text{ deg} \\ \text{with } K' = \frac{1.33|\mu/(\lambda_c + \lambda_i)|}{1.2 + |\mu/(\lambda_c + \lambda_i)|} \quad (\text{III.14})$$

note Without correction to take into account the non-uniformity of the induced velocity, the b_1 calculated was 0.5 deg .

All the results available from my implementation in Simcenter Amesim of the flapping dynamics equation in forward flight are presented Figure 6.

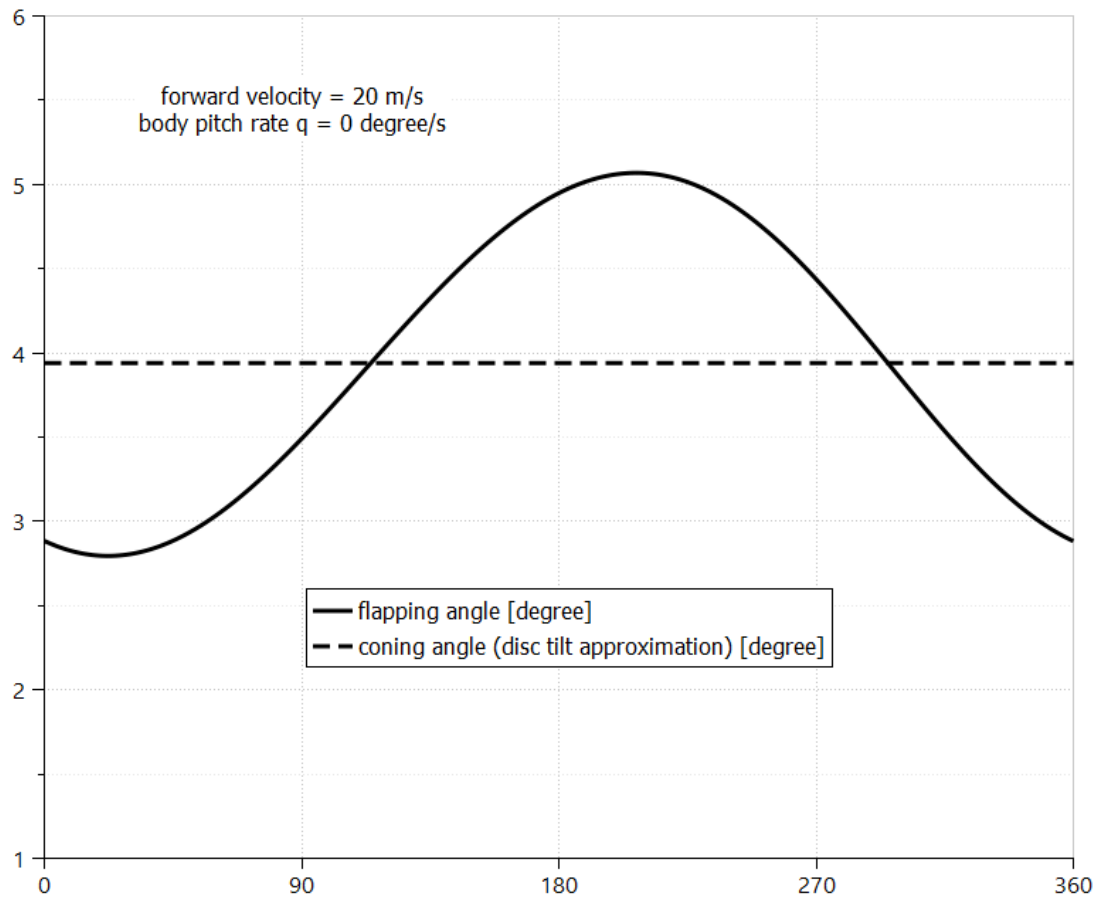


Figure 5: Flapping angle evolution over one revolution for a forward speed $V = 20 \text{ m/s}$

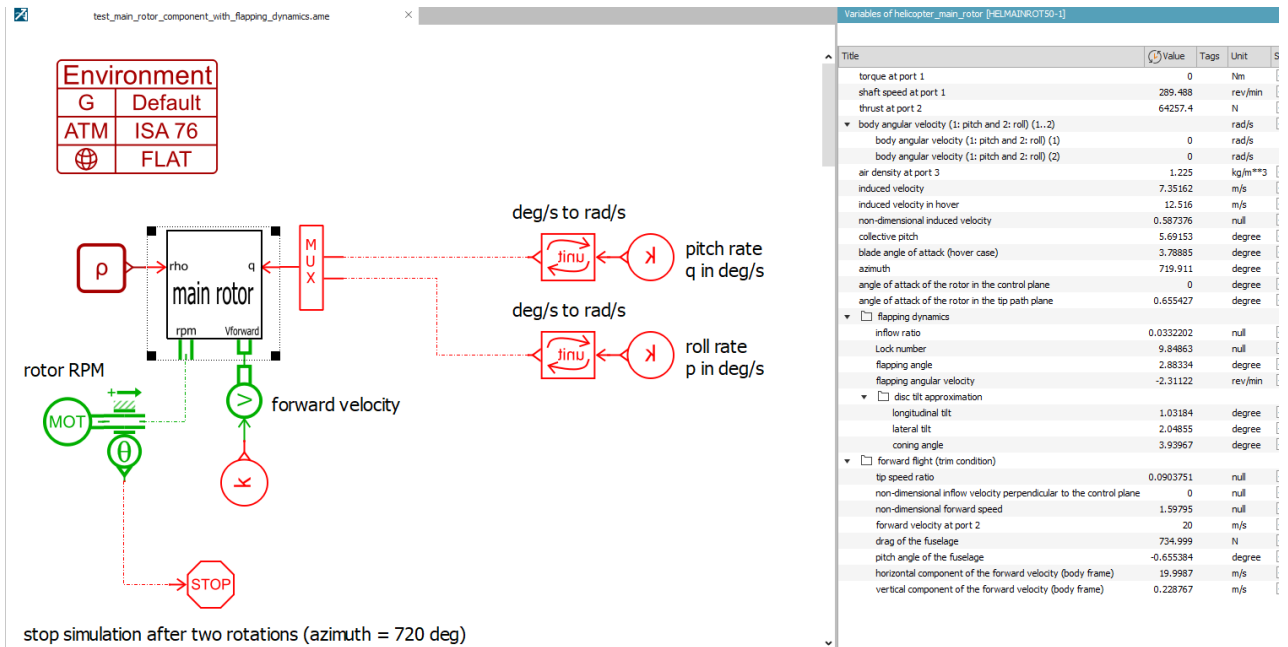


Figure 6: List of variables calculated by the Simcenter Amesim implementation of the flapping dynamics

References

- [vHM02] Th. van Holten and A. Melkert. Helicopter performance, stability and control. faculty of aerospace engineering delft university of technology. AE4-213 lecture notes. Translation and revision of the original Dutch version by Ben Marrant and Marilena Pavel, 2002.

AE4314 Helicopter Performance, Stability and Control
TU Delft online course

sylvain.pluchart@gmail.com

April 2020

Assignment IV

Simulation of a helicopter manoeuvre

1 Helicopter Moment of inertia I_{yy}

1.1 methodology

To compute the AH-64A mass moment of inertia around the pitch axis I_{yy} , I will break down the helicopter into basic geometrical bodies for which the moment inertia calculation is straightforward. Figure 1 shows the bodies selected.

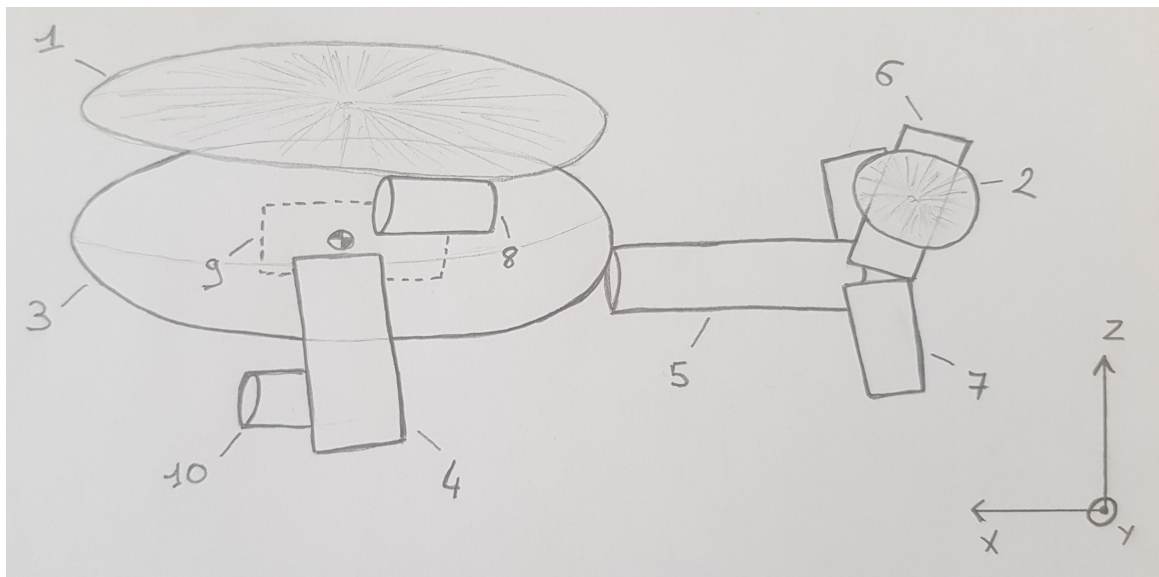


Figure 1: AH-64A breakdown into basic bodies. Numbers refer to Table 1

I will now review the formulas used for the different geometry. These formulas are valid for an axis of rotation passing through the body's center of gravity.

ellipsoid An ellipsoid can be parameterized by its three half-lengths of principal axis. As I am calculating the mass moment of inertia around the pitch axis only (the final objective is to built a *longitudinal* simulator of the helicopter dynamics), only two values in the XZ plane will be required (a and c in Figure 2).

The formula for the mass moment of inertia about is:

$$I_{yy}^{ellipsoid} = \frac{1}{5}m(a^2 + c^2) \quad (\text{IV.1})$$

cylinder Depending on the cylinder orientation I will two formulas:

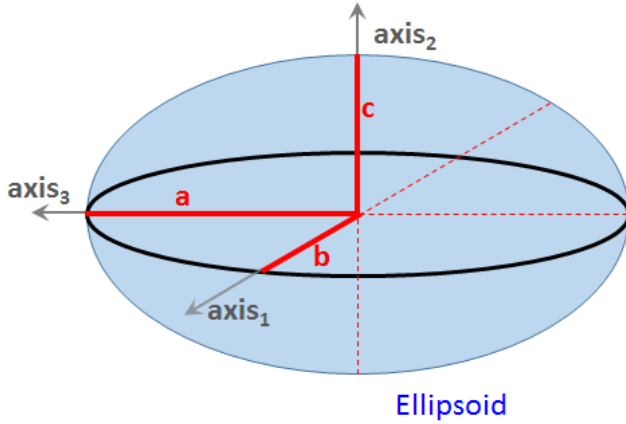


Figure 2: Ellipsoid parameters used in the moment of inertia calculation from vcalc.com

- When the cylinder axis of rotation is parallel to the helicopter pitch axis (tail rotor for example):

$$I_{yy}^{cylinder} = \frac{1}{2}mr^2 \quad (\text{IV.2})$$

- When the cylinder axis of rotation is perpendicular to the helicopter pitch axis (engines for example):

$$I_{yy}^{cylinder} = \frac{1}{12}m(3r^2 + h^2) \quad (\text{IV.3})$$

with r the cylinder radius and h the cylinder length.

solid pad The formula for the mass moment of inertia is:

$$I_{yy}^{solid\ pad} = \frac{1}{12}m(l^2 + h^2) \quad (\text{IV.4})$$

with l and h the two dimensions "contained" in the XY plane.

1.2 calculation for the AH-64A, gross weight 6552 kg

parallel axis theorem The *parallel axis theorem* allows me to calculate the moment of inertia of all the segments about the helicopter pitch axis. I have previously established the moment of inertia about an axis passing through the body's center of gravity. The parallel axis theorem states that if the body rotates about a new axis, which is parallel to the first axis and displaced from it by a distance d , then the moment of inertia I with respect to the new axis is:

$$I_{yy}^{hel} = I_{yy}^{cm} + md^2 \quad (\text{IV.5})$$

with $d = \sqrt{a^2 + b^2}$

Table 1 summarizes the values calculated for the different bodies. The mass values of some segments were found in public data collected for assignment 1 (engine, weapons or fuel for instance). For structural parts (tail boom, wings, and so on) the mass assigned is proportional to volume of the part. a and b are respectively the horizontal and vertical distance between the pitch axis of the helicopter and a parallel axis going through each body's center of gravity.

	segment	type	mass [kg]	d1 [m]	d2 [m]	I_{yy}^{cm} [kgm**2]	a [m]	b [m]	I_{yy}^{hel} [kgm**2]
1	main rotor	cylinder	290	7.3	0.1	3863.8	0	1.9	4910.7
2	tail rotor	cylinder	22	1.4	0.1	21.6	9.1	1.5	1892.9
3	fuselage	ellipsoid	3619	4.6	1.2	16356.1	0	0	16356.1
4	wing	solid pad	188	1.2	0.2	23.2	0	0	23.2
5	tail boom	cylinder	635	0.6	3.8	821.8	5.9	0.6	23169.3
6	vertical tail	solid pad	73	0.8	3.1	62.6	8.8	0.3	5748.2
7	horizontal tail	solid pad	98	1	0.1	8.5	9.1	0	8089.1
8	engines	cylinder	400	0.4	2.5	224.3	1.5	0.6	1268.3
9	fuel	solid pad	727	1	0.9	109.7	0	0	109.7
10	weapons	cylinder	500	0.3	1.9	161.7	0	1	661.7
-	helicopter		6552						62229.2

Table 1: Summary of moment of inertia values calculated. Values of $d1$ and $d2$ depend on the type of body considered as presented in Table 2

	d1	d2
cylinder	radius	height
ellipsoid	half length of the horizontal principal axis	half length of the vertical principal axis
solid pad	length	height

Table 2: Definition of $d1$ and $d2$ for the basic shapes used in the moment of inertia breakdown

2 Trim Calculation

For the trim calculation I will consider an AH-64A with a gross weight of 6552kg flying at Sea Level conditions ($\rho = 1.225 \text{ kg/m}^3$).

2.1 inflow ratio

As derived in the lecture, the inflow ratio λ_i by combining the expression for the thrust coefficient from the Glauert theory and the thrust in trimmed condition:

$$C_{T_{Glauert}} = 2\lambda_i \sqrt{(\mu \sin(\alpha_d) + \lambda_i)^2 + (\mu \cos(\alpha_d))^2} \quad (\text{IV.6})$$

$$T = \sqrt{W^2 + D_{fus}^2} \quad (\text{IV.7})$$

Combining IV.6 and IV.7 gives an equation with λ_i as the only unknown. The symbolic expression for λ_i is too heavy to be copied here. To calculate the value for different forward velocity I used the Wolfram alpha online tool and its *solve* function. Figure 3 shows an example.

The screenshot shows the Wolfram Alpha interface. The input field contains the equation: $2 x \sqrt{(\mu \cos(a))^2 + (\mu \sin(a) + x)^2} = C$ for x , $a=0.0041$, $C=0.00653248$, $\mu=0.054795$. Below the input, the 'solve' button is highlighted. The output section shows the solved variables: $a = 0.0041$, $C = 0.00653248$, $\mu = 0.054795$, and the result $x = 0.0456893$. There are also 'Input interpretation', 'Step-by-step solution', and 'Random' buttons.

Figure 3: Screen capture of the Wolfram Alpha portal used to calculate values of λ_i

2.2 collective and cyclic pitch

In the lecture a system of two equations with two unknowns θ_0 and θ_c has been derived from the expression of:

- the longitudinal flapping angle that equal the cyclic pitch in trimmed condition $a_1 = \theta_c$,
- the thrust coefficient from the Blade Element Theory $C_{T_{BEM}}$,
- and the non-dimensional inflow velocity perpendicular to the control plane λ_c .

I considered this system of equation in its matrix form:

$$\underbrace{\begin{bmatrix} 1 + \frac{3}{2}\mu^2 & -\frac{8}{3}\mu \\ -\mu & \frac{2}{3} + \mu^2 \end{bmatrix}}_A \cdot \begin{bmatrix} a_1 \\ \theta_0 \end{bmatrix} = \underbrace{\begin{bmatrix} -2\mu^2 \frac{D}{W} - 2\mu\lambda_i \\ \frac{4}{\sigma} \frac{C_T}{C_{L_{alpha}}} \mu \frac{D}{W} + \lambda_i \end{bmatrix}}_B \quad (\text{IV.8})$$

After defining two additional matrices $A1$ and $A2$ as the matrix A with respectively the first and the second column replaced by the coefficients of the B matrix, I used the Cramer's rule to solve the system of equation:

$$a_1 = \frac{\det(A1)}{\det(A)} \text{ and } \theta_0 = \frac{\det(A2)}{\det(A)} \quad (\text{IV.9})$$

results The collective and cyclic pitch evolution as a function of the forward velocity V are presented on Figure 4.

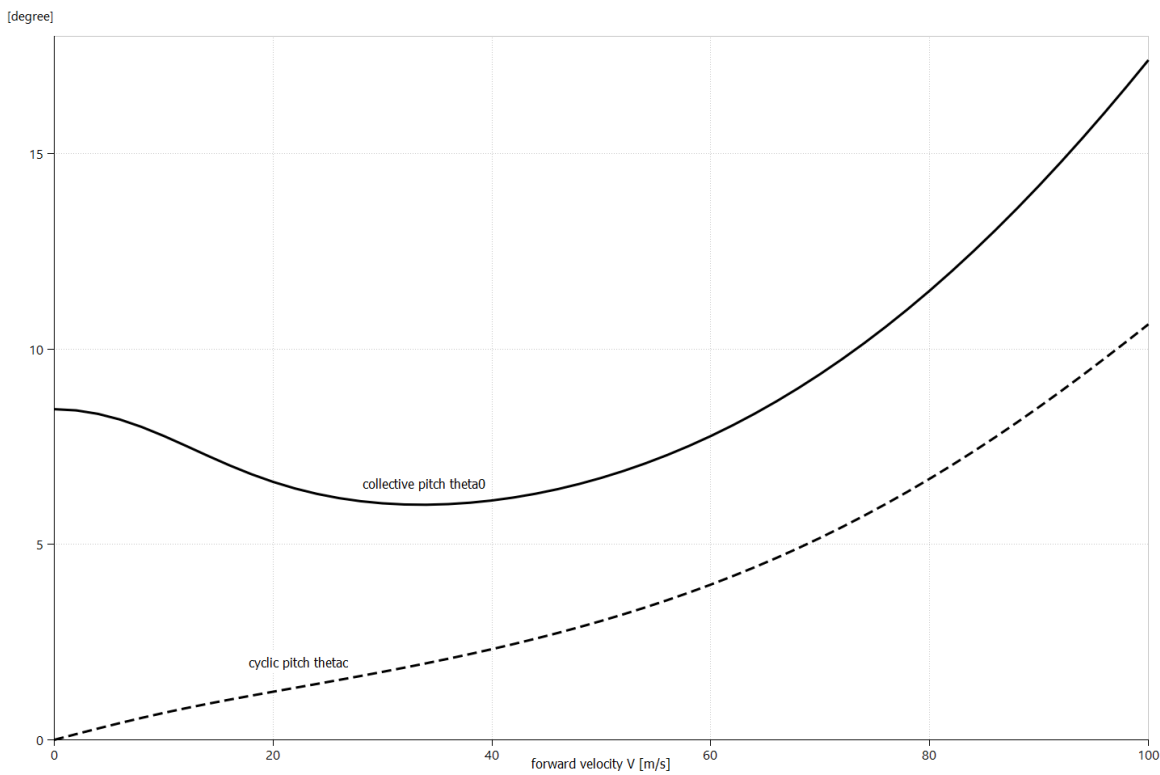


Figure 4: Collective and cyclic pitch positions in trimmed forward flight ($M = 6552 \text{ kg}$ and $\rho = 1.225 \text{ kg/m}^3$)

3 Manoeuvre Simulation

3.1 implementation in Simcenter Amesim

I have implemented the computational scheme of the 3-DoF longitudinal flight equations of dynamics derived during the lecture as a component in Simcenter Amesim . As it was done for the flapping dynamics assignment, I just defined the expressions for the derivatives of the state variables. As a convention these variables contains the *dot* suffix in their name. When running a simulation, the solver will integrate these expressions. The resulting code is presented in Appendix A. Only the statements executed at each integration step are presented. The rest of the code (variable declarations, unit conversion, and so on) is automatically generated by Simcenter Amesim when creating the component, and has been omitted here for the sake of brevity.

induced velocity calculation As suggested in the assignment handout, I considered the induced velocity v_i as a state-variable (instead of solving an implicit scheme at every integration time step). This equation calculates induced velocity derivative on the basis of a "quasi-dynamic inflow":

$$\tau \frac{dv_i}{dt} = C_{T_{BEM}} - C_{T_{Glauert}} \quad (\text{IV.10})$$

velocity quadrant The angle of attack in the control plane is given as:

$$\alpha_c = \theta_c - \epsilon \text{ with } \epsilon = \text{atan}\left(\frac{w}{u}\right) \quad (\text{IV.11})$$

To make the implementation able to handle both forward and backward flights I choose to use the *atan2* variation of the *atan* function. It is part of the C standard library *math.h*. *atan2*(y, x) returns the angle in radians between the positive x-axis of a plane and the point given by the coordinates (x, y). If we consider the plane formed by the helicopter body axis, the origin of that plane being the helicopter CoG, the point of coordinates ($x = u, y = w$) represents one end of the body velocity vector V (see Figure 5). The result of *atan2*(y, x) gives then proper value of ϵ regardless of the flight direction.

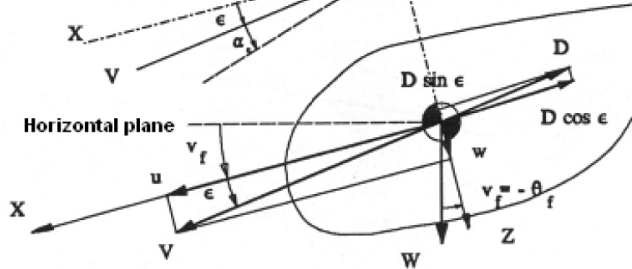


Figure 5: Zoom on the velocity vector definition in the helicopter body frame. From [vHM02]

3.2 hover case

To validate the implementation, I will first run a simulation around an equilibrium position (trim condition), in hover. The Simcenter Amesim sketch is presented in Figure 6 together with the component's parameters corresponding to a hover flight at Sea Level.

remarks on the parameterization

- A non-zero initial value for the vertical velocity w (very small in the hover case) is needed in order to start the integration. This could be improved with a better handling of the $w = 0$ case in the code.
- The initial value for the induced velocity is taken from the previous calculation done on trim condition in Section 2.
- The value of collective pitch has been obtained by trial and error on minimizing the drift in altitude. As expected the value obtained ($\approx 8.3 \text{ deg}$) is close to the one obtained previously in Section 2. Figure 7 shows that trim condition is obtained.

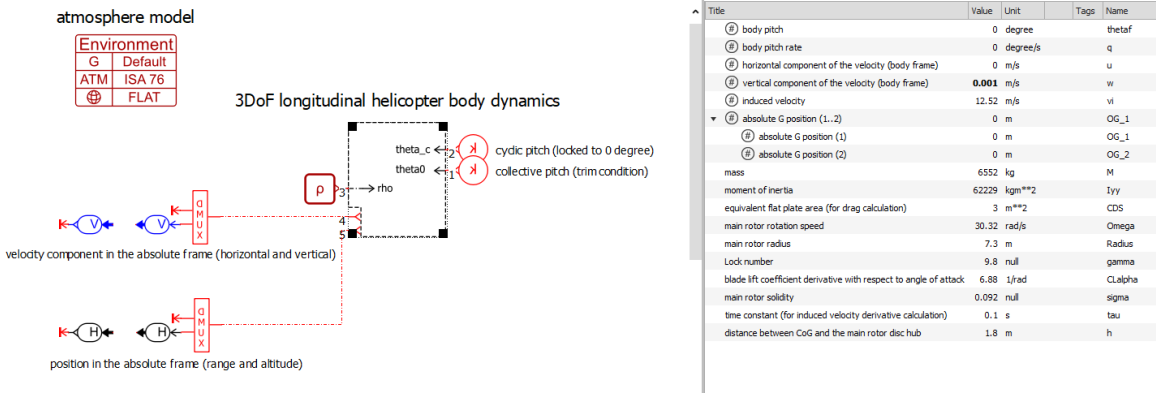


Figure 6: Simcenter Amesim sketch built to test the 3-DoF longitudinal flight component's behavior

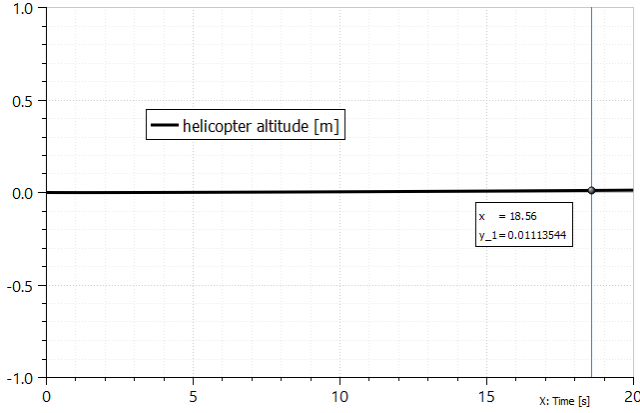


Figure 7: Altitude evolution in the hover case

3.3 simulation of an "altitude-hold" manoeuvre

The next step is to start implementing a controller model. I will first simulate an "altitude-hold" manoeuvre. The cyclic pitch will be kept at a constant value $\theta_c = 0 \text{ deg}$. Starting from hover condition at Sea Level, I will set a target altitude and use the collective pitch command to reach it.

collective pitch control loop The controller is made of two cascaded controllers that implement the following logic, as proposed in the assignment handout:

1. The target altitude h_{des} is compared with the current altitude h to compute a positioning error.
2. This error on position is multiplied by a fixed gain K_3 to compute a velocity setpoint.
3. The target vertical velocity c_{des} is then compared with the current vertical velocity c to compute a velocity error.
4. This error on velocity is multiplied by a gain K_1 . The integral of that error is also computed and multiplied by another gain K_2 . Both components are added to compute an increment in collective pitch $d\theta_0$.
5. The increment is added to an average control position $\theta_{0_{gen}}$ to compute the collective pitch setpoint. This average control value will be taken as the trim condition for the initial state of the helicopter.
6. A time-delay in applying the command, modeled as a first order lag, is added. It is added for two reasons:
 - Without it there would be an implicit loop in the system of equation. Because the helicopter's altitude and velocity depend on the collective pitch, that itself depends on the helicopter's altitude and velocity through the control loop I have implemented.
 - In the real system the change in collective pitch would not be instantaneous. Because for instance the actuators have their dynamics (not modeled here).

These different steps can be summarized by Expression IV.12 and the Simcenter Amesim implementation presented on Figure 8.

$$\begin{cases} c_{des} = K_3(h_{des} - h) \\ \theta_0^{command} = \theta_{0_{gen}} + d\theta_0 \text{ with } d\theta_0 = K_1(c_{des} - c) + K_2 \int (c_{des} - c) dt \end{cases} \quad (\text{IV.12})$$

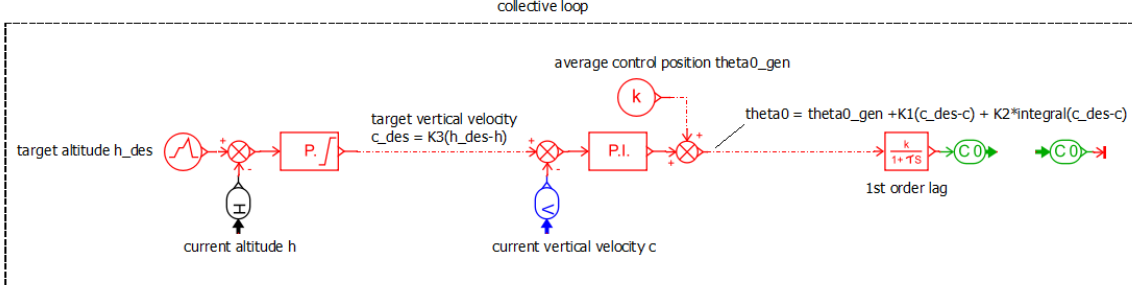


Figure 8: Implementation in Simcenter Amesim of the collective pitch control loop

note on the velocity setpoint I have added upper and lower limits in the velocity setpoint calculation to account for the actual performance of the AH-64A helicopter. I used the value of maximum vertical rate of climb found in the literature (762 m/min at Sea Level in the configuration considered).

simulation results The simulation consists of an initial hover for 5 seconds at $h = 0 \text{ m}$. Then the altitude setpoint is changed to a constant value of $h = 100 \text{ m}$. Figure 9 shows the helicopter altitude, vertical velocity and collective pitch evolutions in response to that command.

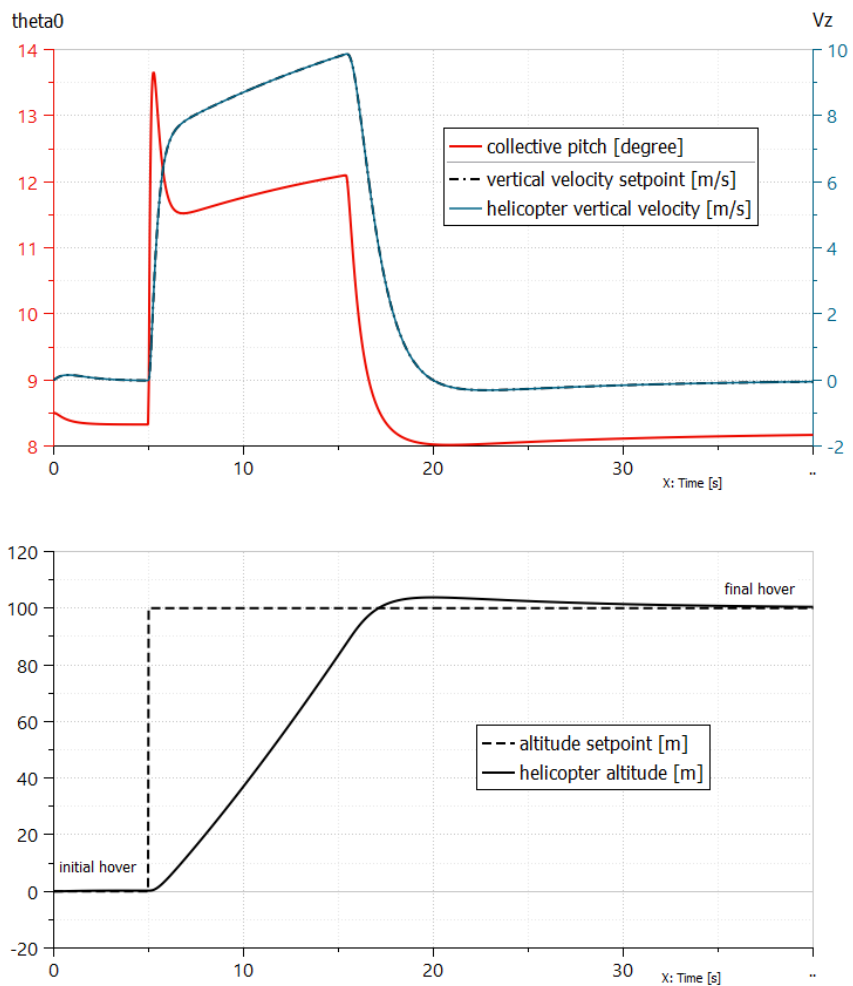


Figure 9: AH-64A 3-DoF non-linear longitudinal model response to a change in altitude setpoint.
 $K_1 = 0.5 \text{ } 1/s$, $K_2 = 0.05 \text{ rad/m}$ and $K_3 = 1 \text{ (s.rad/m)}$

3.4 ADS-33 manoeuvre

longitudinal cyclic pitch control loop As I did for the collective pitch control for the altitude-hold simulation, I implemented a control loop for the longitudinal cyclic. The controller's architecture consists of a PID that takes a body pitch error as an input and computes a corresponding cyclic pitch command. The implementation is summarized with the Expression IV.13. A graphical representation is presented on the Simcenter Amesim screen capture of the complete model Figure 10.

$$\theta_c^{command} = K_4(\theta_{fdes} - \theta_f) + K_5 \frac{d(\theta_{fdes} - \theta_f)}{dt} + K_6 \int (\theta_{fdes} - \theta_f) dt \quad (\text{IV.13})$$

remark on the controller implementation To perform the manoeuvre I need to set target airspeeds to the helicopter model. I have defined the corresponding body pitch setpoint from the trim conditions established in Section 2. I could have added another loop in the controller that would take the airspeed error as an input and would calculate a body pitch setpoint. This would model what the pilot is consciously doing by looking at the airspeed on his instruments, and pitching the helicopter body to increase or decrease that speed.

simulation results The results presented Figure 11 show that our helicopter model can perform the ADS-33 manoeuvre with performance standards within the "adequate" ranges (altitude within ± 200 ft, trim hands-off airspeed within ± 5 knots, change from one airspeed to the other < 2 min and heading maintained within ± 10 deg). It is important to note that the controllers are not optimized. I will not draw any conclusion on the AH-64A performance based on these simulation results. The objective here is to get an idea of how the manoeuvre would be handled by the pilot.

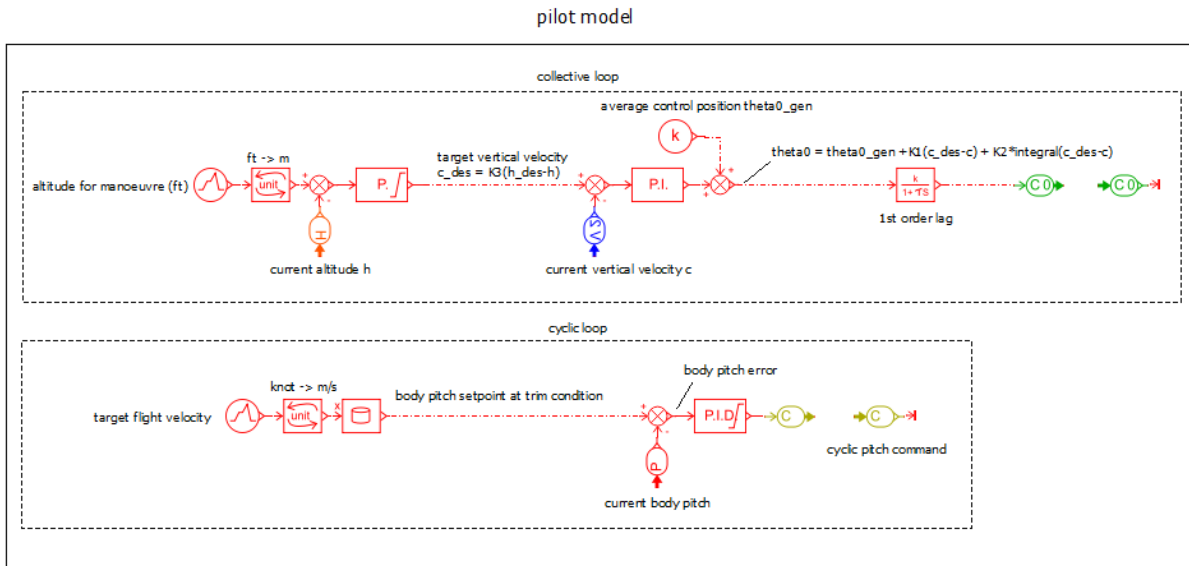


Figure 10: Simcenter Amesim sketch of the complete simulator of the ADS-33 manoeuvre

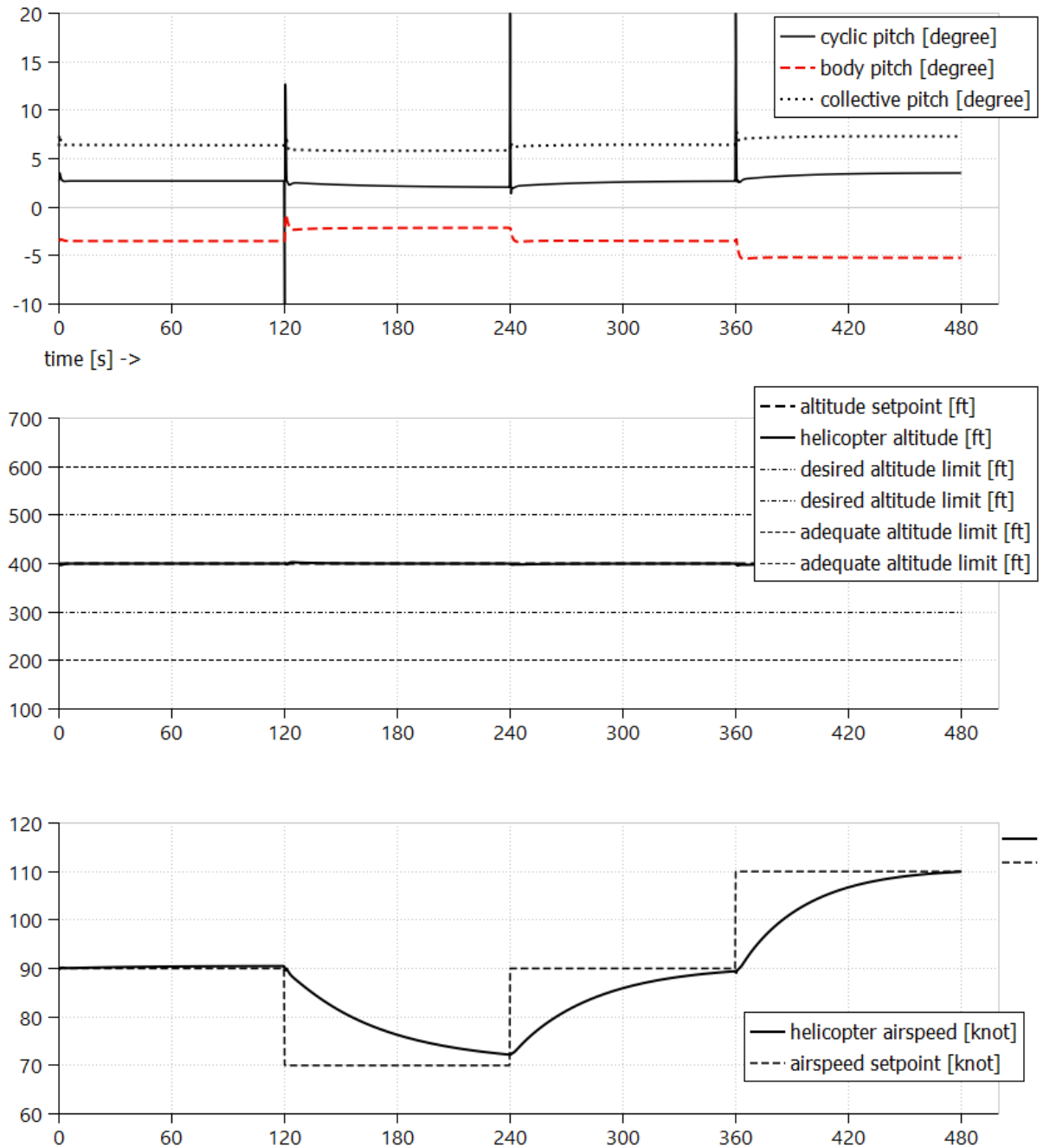


Figure 11: Results of speed control manoeuvre of the ADS-33 simulation performed at 400 *ft* altitude.
 $K_4 = -2$, $K_5 = -2$ s and $K_6 = -0.2$ 1/s (all other gains are kept unchanged).

discussion on how the pilot is "flying" the manoeuvre A zoom on how the helicopter model decelerates from trimmed level flight at 90 knots to 70 knots and retrim for hands-off flight is presented Figure 12. We recognize the behavior of an acceleration control system. First the cyclic pitch is set to a negative value in order to build up a positive body pitch rate. As the body pitch increases, the cyclic pitch takes then an opposite value to reduce the body pitch rate. This way it slows down the motion to make sure that the body will reach its final pitch angular position. The cyclic pitch is then going back to its final trimmed condition value.

It follows the analogy of a ball rolling on a tilting plate presented in the lecture, which is similar to an inverted pendulum. You first build up some velocity to move the ball on one side by tilting the plate (we have a non-zero acceleration). When the ball is close enough to its target position, tilting the plate in the opposite direction will reduce the ball velocity (the acceleration takes the opposite sign), and make sure that when it reaches its final position we will have $velocity = acceleration = 0$.

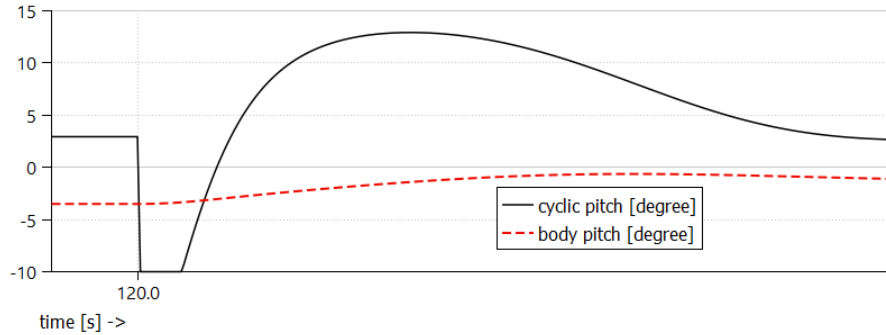


Figure 12: Cyclic pitch control to achieve a change in the helicopter body pitch (manoeuvre to decelerate from 90 knots to 70 knots airspeed)

4 Stability

4.1 phugoid mode at 90 knots with no controller

The helicopter 3-DoF longitudinal model results show the oscillatory exchange between altitude and horizontal velocity u . When no controller is plugged to the body dynamics models, this mode is unstable (Figure 13).

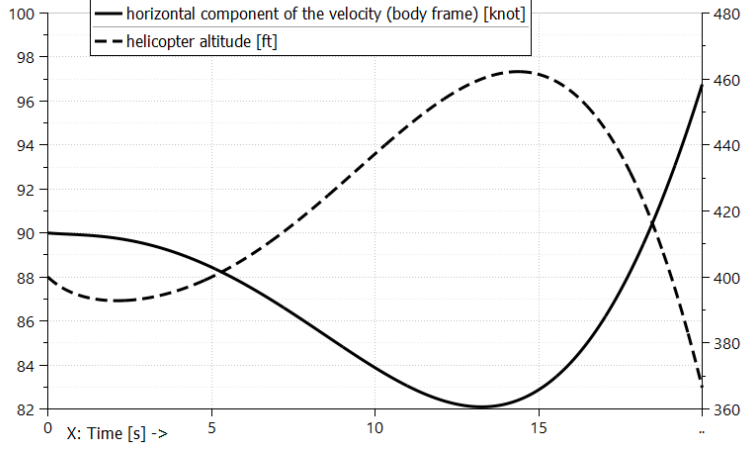


Figure 13: Phugoid mode illustrated with the altitude-velocity oscillatory exchange (one period represented).
3 DoF-longitudinal model with no controller.

4.2 phugoid mode at 90 knots with PID controller

When looking at the same variables on the simulator and its controller, the one used to run the ADS-33 manoeuvre, I see that the model frequency and damping characteristics have changed (Figure 14). The motion is now rapidly damped, its frequency is higher.

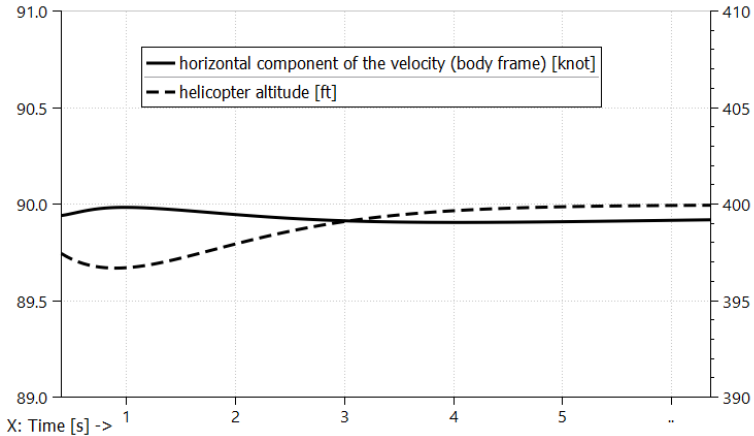


Figure 14: Phugoid mode illustrated with the altitude-velocity oscillatory exchange (one period represented).
3 DoF-longitudinal model with its controllers.

4.3 comparison of frequency and damping

In this section I will use the linear analysis toolset of Simcenter Amesim to calculate numerically the stability derivatives. The frequency and damping characteristics of both versions of the simulator are compared in Table 3

	simulator with no controller	simulator with PID controller
frequency [Hz]	0.04	0.20
damping [%]	-51.1	86.1
eigenvalue real part	0.13	-1.08

Table 3: Comparison of the phugoid mode characteristic of the two simulators.

A 3-DoF longitudinal dynamics implementation

```

/* >>>>>>>>>>>> Calculation Function Executable Statements. */

*epsilon = atan2(*w, *u); // to monitor the quadrant the helicopter flies in.

*V = sqrt(pow(*u, 2) + pow(*w, 2));

*alphac = *thetac - *epsilon; // TODO(Sylvain): handle the *w = 0 case properly.

*mu = (*V * cos(*alphac)) / (Omega * Radius);

*lambda_dac = (*V * sin(*alphac)) / (Omega * Radius);

*lambda_dai = *vi / (Omega * Radius);

*a1 = (((-16.0 * *q) / (gamma * Omega)) + ((8.0/3.0) * *mu * *theta0) - (2.0 * *
    mu * (*lambda_dac + *lambda_dai)))
/ (1.0 - (1.0/2.0) * pow(*mu, 2));

// thrust coefficients
*CTelement = CLalpha * (sigma/4.0) * ((2.0/3.0) * *theta0 * (1.0 + (3.0/2.0) *
    pow(*mu, 2)) - (*lambda_dac + *lambda_dai));
*CTGlauert = 2.0 * *lambda_dai * sqrt( pow((*V / (Omega * Radius)) * cos(*alphac -
    *a1), 2) + pow((*V / (Omega * Radius)) * sin(*alphac - *a1) + *lambda_dai, 2) );

// thrust force
*Thrust = *CTelement * *rho * pow(Omega * Radius, 2) * M_PI * pow(Radius, 2);

// drag force
*Dfus = (1.0/2.0) * *rho * CDS * pow(*V, 2);

// equations of motion

// dvi/dt calculation dvi/dt on the basis of a 'quasi dynamic inflow'
*vidot = (*CTelement - *CTGlauert) / tau;

*u_dot = -g * sin(*thetaf) - ((*Dfus * *u) / (M * *V)) + (*Thrust/M) * sin(*thetac -
    *a1) - *q * *w;

*w_dot = g * cos(*thetaf) - ((*Dfus * *w) / (M * *V)) - (*Thrust/M) * cos(*thetac -
    *a1) + *q * *u;

*q_dot = -(*Thrust/Iyy) * h * sin(*thetac - *a1);

*thetaf_dot = *q;

// velocity and position in the absolute frame
vG[0] = *V * cos(*epsilon - *thetaf); // horizontal
vG[1] = - *V * sin(*epsilon - *thetaf); // vertical

OGdot[0] = vG[0];
OGdot[1] = vG[1];

/* <<<<<<<<<End of Calculation Executable Statements. */

```

References

- [vHM02] Th. van Holten and A. Melkert. Helicopter performance, stability and control. faculty of aerospace engineering delft university of technology. AE4-213 lecture notes. Translation and revision of the original Dutch version by Ben Marrant and Marilena Pavel, 2002.